Macromolecules

Article

How Are Insoluble Blocks Interacted with and Packed Inside a Micelle Made of Block Copolymers in a Selective Solvent?

Liangzhi Hong, Fan Jin, Junfang Li, Yijie Lu, and Chi Wu

Macromolecules, **2008**, 41 (21), 8220-8224 • DOI: 10.1021/ma801702t • Publication Date (Web): 10 October 2008

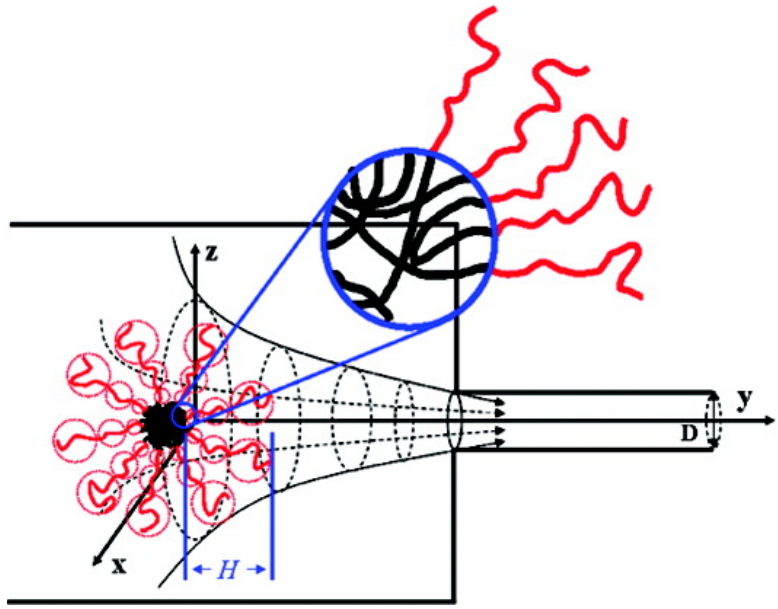

More About This Article

Additional resources and features associated with this article are available within the HTML version:

- Supporting Information
- Access to high resolution figures
- Links to articles and content related to this article
- Copyright permission to reproduce figures and/or text from this article

View the Full Text HTML

Macromolecules is published by the American Chemical Society. 1155 Sixteenth Street N.W., Washington, DC 20036

How Are Insoluble Blocks Interacted with and Packed Inside a Micelle Made of Block Copolymers in a Selective Solvent?

Liangzhi Hong,[†] Fan Jin,[†] Junfang Li,[‡] Yijie Lu,[‡] and Chi Wu*[,†,‡]

Department of Chemistry, The Chinese University of Hong Kong, Shatin, N. T., Hong Kong, and Hefei National Laboratory of Physical Science at Microscale, Department of Chemical Physics, University of Science and Technology of China, Hefei, Anhui, 230026, China

Received July 28, 2008; Revised Manuscript Received August 15, 2008

ABSTRACT: It is well-known that block copolymers can form large core−shell micelles in a selective solvent. The ultrafiltration of such polymeric micelles made of polystyrene (PS) and polyisoprene (PI) block copolymers in *n*-hexane through small pores (20 nm) is possible only when the flow-rate-dependent hydrodynamic force in the range 10^{-15} to 10^{-12} N (i.e., 1 fN−1 pN) is sufficiently strong to pull individual copolymer chains out of the core and disintegrate each micelle. Therefore, we are able to find how strong insoluble PS blocks in the core interact with each other from such a critical flow rate. Our results reveal that the micelle retention gradually decreases as the flow rate increases, different from a sharp first-order coil-to-stretch transition of a flexible linear homopolymer chain under the same elongation flow field. As expected, the interaction strength increases as the PS block becomes longer. Each flow-rate dependence of the micelle retention can be converted to a hydrodynamic force distribution $f(F_h)$. For PS-*b*-PI diblock copolymers, $f(F_h)$ has a single peak in the range 1−200 fN, whereas for PI-*b*-PS-*b*-PI triblock copolymers, there are two separated peaks in $f(F_h)$, respectively, in the ranges 3−20 and 30−500 fN, attributing to two kinds of packing of the PS blocks inside the core; namely, the packing of unentangled and entangled insoluble PS blocks.

Introduction

The micellization of block copolymers in a selective solvent to form some core−shell nanostructures has been extensively studied because of their potential applications, such as in cosmetics, emulsification, drug delivery, and environmental purification.[1−4] However, some basic questions are still unanswered, including how each micelle is dynamically equilibrated with individual copolymer chains (unimers) free in the solution and how the insoluble blocks are packed and interact with one another inside the core. It is rather difficult, if not impossible, to separate polymeric micelles from unimers and characterize how much force is needed to pull individual chains out of a micelle floating inside a solution.[5−7]

On the other hand, ultrafiltration has been routinely used to separate different components of a polydisperse system.[8−16] Recently, using a special double-layer membrane with small pores, we successfully observed the predicted discontinued first-order coil-to-stretch transition in the ultrafiltration of flexible linear homopolymer chains.[17] Namely, the chains can pass through a pore much smaller than its unperturbed size only when the flow rate reaches a critical value. Note that, in the ultrafiltration, the microscopic flow velocity in each small pore is much higher than that of the macroscopic one because the total cross section of all the pores is only a small fraction of the surface area of a membrane. For each pore with a convergent flow, there exists a large elongational gradient at its entrance. The strain rate (ε) under such a gradient is related to the microscopic flux inside the pore (q) as

$$\varepsilon(r) = \frac{\partial v_y}{\partial r} \approx \frac{J}{r^3} \propto \frac{D^2}{4r^3} q \qquad (1)$$

where J is the microscopic flow rate inside the pore, v_y is the velocity in the direction perpendicular to the membrane surface, D is the pore diameter, and $0 < r < D/2$, a distance away from the center line of the pore.[18]

For polymeric micelles with a size much larger than the pore, we can imagine that only one or few "arms" could enter the pore with no flow or under a very low flow rate. In this way, the micelle is stuck at the entrance of the pore, as shown in Figure 1. Each lyophilic block can be visualized as a chain tethered on the lyophilic/lyophobic interface with a stretched conformation and made of a string of correlated blobs.[19−23] Under an elongational flow, the Stocks hydrodynamic force for each blob is $\eta v \zeta$, where η, v, and ζ are the solvent viscosity, the flow velocity, and the blob size, respectively. The hydrodynamic force (F_h) on each lyophilic block (arm) is the sum of the hydrodynamic force on all the blobs in one arm, that is, $\eta v H$, where H is the length of the arm along the flow direction and $v = J/D^2$.

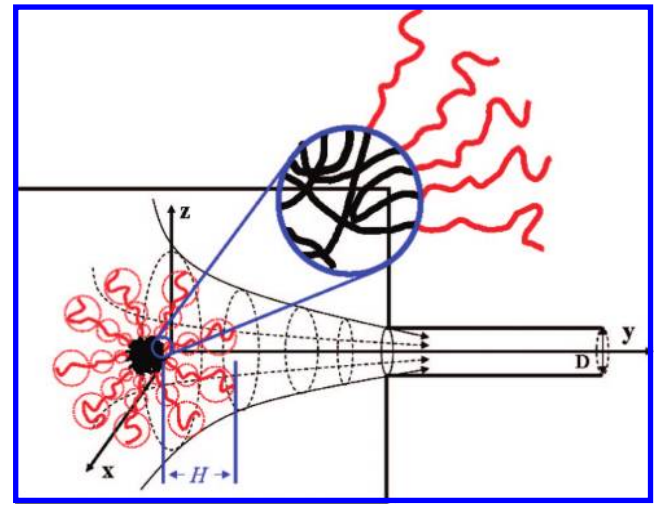

Figure 1. Schematic of ultrafiltration of a polymeric core−shell micelle made of block copolymer chains through a smaller pore under an elongational flow. The enlarged picture shows different kinds of chain packing of insoluble blocks in the core.

* Corresponding author. E-mail: chiwu@cuhk.edu.hk.
[†] The Chinese University of Hong Kong.
[‡] University of Science and Technology of China.

10.1021/ma801702t CCC: $40.75
Published on Web 10/10/2008

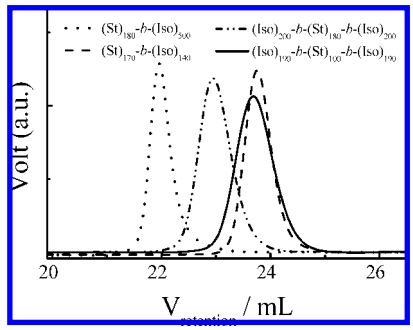

Figure 2. SEC graph of two triblock and two diblock copolymers, where THF is used as the eluent.

It is not hard to further imagine that each micelle could pass through a smaller pore only when individual copolymer chains were pulled out and the micelle is disintegrated. Therefore, it is possible to estimate the strength of interaction among different insoluble blocks in the core from the hydrodynamic force required to rupture polymeric micelles. Note that such interaction strength is vitally important in the rheological study of suspensions stabilized by polymer chains, where a layer of polymer chains absorbed on the particle surface prevents the interparticle aggregation.[23] If all the insoluble blocks were interacted with in an identical way, there would exist only one critical flow rate. In reality, the interaction among different insoluble blocks in the core should be different so that we expect a distribution of the hydrodynamic force, $f(F_h)$. In the current study, we measured the flow-rate-dependent retention of large polymeric micelles through smaller pores and answered how strongly the insoluble blocks interacted with one another and packed inside the core.

Experimental Section

Materials. Two polystyrene-*b*-polyisoprene (PS-*b*-PI) diblock copolymers, $(St)_{180}$-*b*-$(Iso)_{500}$ and $(St)_{170}$-*b*-$(Iso)_{140}$, were synthesized using high-vacuum living anionic polymerization initiated by *sec*-butyllithium in cyclohexane at 45 °C. Two PI-*b*-PS-*b*-PI triblock copolymers, $(Iso)_{200}$-*b*-$(St)_{180}$-*b*-$(Iso)_{200}$ and $(Iso)_{190}$-*b*-$(St)_{100}$-*b*-$(Iso)_{190}$, were synthesized using high-vacuum living anionic polymerization initiated by potassium naphthalenide in THF at −78 °C. The synthetic details were well-documented in literature.[24−28] Note that PI blocks synthesized at different solvents and temperatures have very different microstructures; namely, most isoprene monomers are connected via positions 1 and 4 in cyclohexane, but via positions 3 and 4 in THF. For a given degree of polymerization, the 1,4 connection leads to a longer chain. This has to be considered when we calculate the hydrodynamic force later. The resultant block copolymers were characterized by size exclusion chromatography (SEC) with a multiangle laser light scattering detector, a combination of static and dynamic laser light scattering, and proton nuclear magnetic resonance. Such prepared four block copolymers are narrowly distributed, as shown in Figure 2, with a polydispersity index in the range 1.05−1.08.

Ultrafiltration. An SGE gastight syringe and a Whatman 0.02-μm filter were used. The double-layer structure of the membrane was well-characterized.[17,29] The upper thick layer (59 μm) and the under thin layer (1 μm), respectively, contain 200- and 20-nm pores. On average, each small pore is covered by a large pore. The whole setup of the ultrafiltration experiments was performed inside an SI 60D incubator so that the solution was maintained at a desired temperature. The flow rate of each micelle solution through the filter was controlled by a Harward-2000 syringe pump. The micelle solutions were prepared by directly dissolving each block copolymer in *n*-hexane, a solvent selectively good for PI. The micelle solutions were kept at 50 °C for 3 days to ensure that a dynamic equilibrium between individual chains (unimers) and micelles was well-established. The micelle solutions before and after the filtration were analyzed by a combination of static and dynamic laser light scattering (LLS).

Laser Light Scattering. A commercial LLS spectrometer (ALV/DLS/SLS-5022F) equipped with a multi-τ digital time correlator (ALV5000) and a cylindrical 22 mW He−Ne laser ($\lambda_0 = 632$ nm, Uniphase) as the light source was used. Note that, for block copolymers with a very low critical micelle concentration (CMC), the time-average scattering intensity $\langle I \rangle$ is dominantly from large self-assembled polymeric micelles. The retention ratio ($R(\%)$) of polymeric micelles by small pores can be calculated from the micelle concentrations ($C_{mic,0}$ and C_{mic}) before and after the ultrafiltration, which are related to $\langle I \rangle$.

In static LLS,[30] $\langle I \rangle$ is proportional to the product of molar mass (M) and concentrations (C) of a scattering object, that is, $\langle I \rangle \approx MC$. For a given polymer/solvent system under identical experimental conditions, $M_{micelle}$ is a constant. Therefore,

$$R(\%) = \frac{C_{mic,0} - C_{mic}}{C_{mic,0}} \times 100\% = \frac{\langle I \rangle_{mic,0} - \langle I \rangle_{mic}}{\langle I \rangle_{mic,0}} \times 100\% \cong \frac{\langle I \rangle_0 - \langle I \rangle}{\langle I \rangle_0} \times 100\% \quad (2)$$

where $\langle I \rangle_o$ and $\langle I \rangle$ are the total time-average scattering intensities before and after the ultrafiltration, respectively.

In dynamic LLS,[31] the Laplace inversion of each measured intensity−intensity time correlation function $G^{(2)}(q,t)$ in the self-beating mode can lead to a characteristic relaxation-time distribution $G(\tau)$. In this study, the CONTIN program in the correlator was used. For a pure diffusive relaxation, τ is related to the translational diffusion coefficient D by $(1/\tau q^2)_{C\to 0, q\to 0} \to D$. Therefore, $G(\tau)$ can be converted into a transitional diffusion coefficient distribution $G(D)$ or further to a hydrodynamic radius distribution $f(R_h)$ by using the Stokes−Einstein equation, $R_h = (k_B T/6\pi\eta)/D$, where k_B, T, and η are the Boltzmann constant, the absolute solution temperature, and the solvent viscosity, respectively. If $G(\tau)$ has more than one peak, the area (A) under each peak is proportional to the average scattering intensity ($\langle I \rangle$) from its corresponding scattering objects. In a proper solution mixture of micelles and unimers with a relatively higher CMC, we expect one micelle peak and one unimer peak. The area ratio of these two peaks (A_{mic}/A_{uni}) equals the ratio of two corresponding scattering intensities ($\langle I \rangle_{mic}/\langle I \rangle_{uni}$). For a given polymer solution, $\langle I \rangle_{uni}$ ($\propto C_{uni}M_{uni}$) is a constant, independent of the polymer concentration (C) as long as C is higher than CMC, where C_{uni} and M_{uni} are the concentration and molar mass of unimers, respectively. Therefore,

$$R(\%) = \frac{\langle I \rangle_{mic,0} - \langle I \rangle_{mic}}{\langle I \rangle_{mic,0}} \times 100\% = \left(\frac{\frac{\langle I \rangle_{mic,0}}{\langle I \rangle_{uni,0}} - \frac{\langle I \rangle_{mic}}{\langle I \rangle_{uni,0}}}{\frac{\langle I \rangle_{mic,0}}{\langle I \rangle_{uni,0}}} \right) \times 100\% = \left(\frac{\frac{A_{mic,0}}{A_{uni,0}} - \frac{A_{mic}}{A_{uni}}}{\frac{A_{mic,0}}{A_{uni,0}}} \right) \times 100\% \quad (3)$$

Results and Discussion

We started with the ultrafiltration of polymeric micelles made of two PS-*b*-PI diblocks in *n*-hexane. Figure 3 shows that polymeric micelles made of $(St)_{180}$-*b*-$(Iso)_{500}$ and $(St)_{170}$-*b*-$(Iso)_{140}$ are narrowly distributed in *n*-hexane. The CMC values of these two diblock copolymers in *n*-hexane are so low that unimers are not detectable in laser light scattering. It is helpful

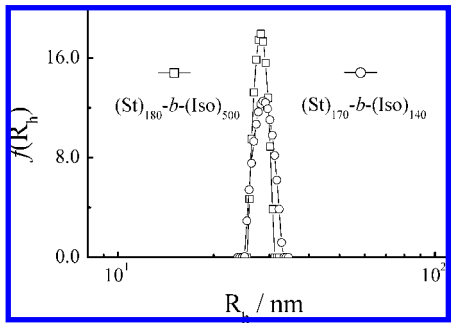

Figure 3. Hydrodynamic radius distributions $f(R_h)$ of polymeric core−shell micelles made of $(St)_{180}$-b-$(Iso)_{500}$ and $(St)_{170}$-b-$(Iso)_{140}$, where $C = 5.0 \times 10^{-5}$ g/mL and $T = 25.0$ °C.

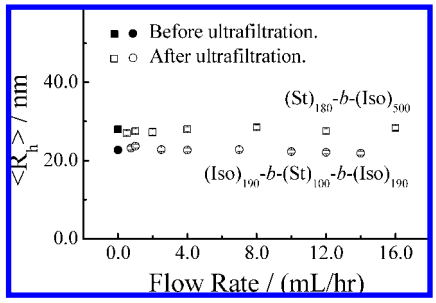

Figure 4. Flow-rate dependence of average hydrodynamic radius ($\langle R_h \rangle$) of polymeric micelles made of $(St)_{180}$-b-$(Iso)_{500}$ and $(Iso)_{190}$-b-$(St)_{100}$-b-$(Iso)_{190}$ after ultrafiltration. For comparison, $\langle R_h \rangle$ values before ultrafiltration are also plotted.

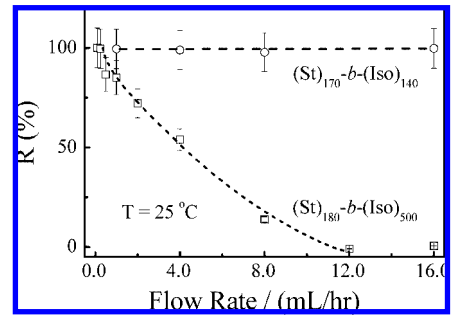

Figure 5. Macroscopic flow rate dependence of retention ratio of polymeric micelles made of $(St)_{180}$-b-$(Iso)_{500}$ and $(St)_{170}$-b-$(Iso)_{140}$ in n-hexane.

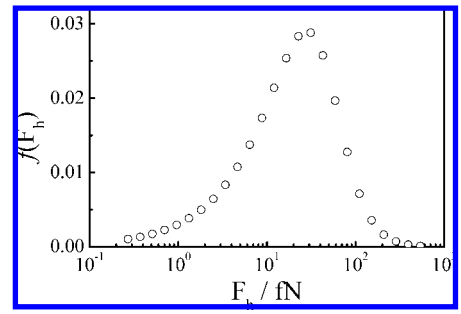

Figure 6. Distribution of hydrodynamic force ($f(F_h)$) required to rupture polymeric micelles made of $(St)_{180}$-b-$(Iso)_{500}$ in n-hexane at 25.0 °C.

to note that the radius of the micelle core (R_c) is scalable to the copolymer composition (i.e., $R_c^{-1} \propto m/n$, where m and n, respectively, are the numbers of repeating units of soluble and insoluble blocks in a A_mB_n- or $A_mB_nA_m$-type block copolymers).[32] Keeping the insoluble PS block length nearly identical, the core size increases, but the shell thickness decreases, as the soluble PI block length becomes shorter. The two effects are opposite on the overall size of polymeric core−shell micelles. This might explain why polymeric micelles made of $(St)_{180}$-b-$(Iso)_{500}$ and $(St)_{170}$-b-$(Iso)_{140}$ have a similar size. It is clear that polymeric micelles made of two PS-b-PI copolymers are larger than the pore size (20 nm) and narrowly distributed in size.

To pull individual chains out of each micelle, we have to consider the mobility of insoluble blocks in the core. Such chain mobility has been studied by different methods, including fluorescence techniques[33−35] and NMR.[36,37] The so-called "frozen-in" micelles can form in both aqueous and organic solutions with a "glassy" core,[38,39] in which the exchange between polymer chains free in the solution (unimres) and entrapped inside the micelle is very slow. On the other hand, it has been known that a fully collapsed linear chain in a poor solvent still contains ~70% of solvent in its hydrodynamic volume.[40] Therefore, the insoluble core is not as dry as and as glassy as one normally thought. Antonietti et al.[41] reported that the shear force generated in a common viscometer tube could disintegrate polymeric micelles made of block copolymers. Jones et al.[42] also showed that a weak shear flow could affect the micelle formation of diblock copolymers in selective solvents. In our current ultrafiltration experiments, polymeric micelles are broken and individual chains are pulled through small pores. Figure 4 shows that, after ultrafiltration, excess unimers quickly reassemble into polymeric micelles with a similar average hydrodynamic radius ($\langle R_h \rangle$) size as long as the copolymer concentration in the effluent is higher than its CMC.

Figure 5 shows the flow-rate dependence of the retention ratio of polymeric micelles made of $(St)_{180}$-b-$(Iso)_{500}$ and $(St)_{170}$-b-$(Iso)_{140}$. For $(St)_{170}$-b-$(Iso)_{140}$, polymeric micelles are completely retained by the filter. We were not able to break them even at the maximum flow rate 100 mL/h available in our current setup because the soluble PI block is too short. For $(St)_{180}$-b-$(Iso)_{500}$, the retention of polymeric micelles continually decreases as the flow rate increases after the flow rate is higher than a threshold of 0.25 mL/h, indicating that individual copolymer chains are pulled out of each micelle.

It should be stated that the typical time to complete one ultrafiltration experiment is about 10−15 min, but the formation of polymeric micelles from individual chains is nearly instant. The question is how long it takes for the exchange between polymer chains inside the micelle and unimers free in the solution under no flow (i.e., the dynamic equilibrium time). A few years ago, we studied the merging kinetics of two kinds of polymeric micelles and found that it normally takes a few hours for the exchange between the chains inside polymeric micelles and unimers free in the solution.[43] Therefore, most of the copolymer chains pulled through small pores in the ultrafiltration are from the broken micelles, not unimers free in the solution. Our result also shows that within a few hours no micelle is detected on the other side of the membrane if there is no flow.

Note that the flow rate is directly related to the Stokes hydrodynamic force (F_h) generated from the elongational flow field on the soluble PI block; namely, $F_h = \eta HJ/D^2$, where H is the chain extension along the flow field, as shown in Figure 1. After taking a differentiation of the retention ratio in Figure 5, we are able to obtain a distribution of the hydrodynamic force [$f(F_h)$] required to disintegrate polymeric micelles. $f(F_h)$ directly reflects the strength distribution of the interaction among different insoluble PS blocks inside the core. Figure 6 shows such a hydrodynamic force distribution for $(St)_{180}$-b-$(Iso)_{500}$ in n-hexane at 25.0 °C. $f(F_h)$ has only one peak with an average hydrodynamic force of ~30 fN. As expected, here each PS block is collapsed and then interacts with one another in the core via the van der Waals force.

The situation should be different for an A-B-A triblock copolymer in a solvent selectively good for the two A blocks.

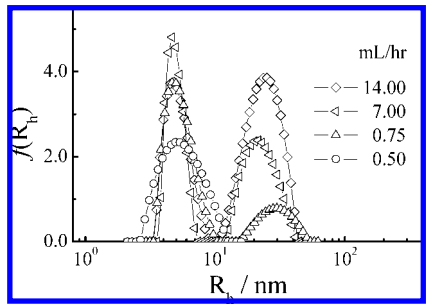

Figure 7. Macroscopic flow-rate dependence of hydrodynamic radius distribution ($f(F_h)$) of $(Iso)_{190}$-*b*-$(St)_{100}$-*b*-$(Iso)_{190}$ solution in *n*-hexane after the ultrafiltration, where $C = 6.0 \times 10^{-4}$ g/mL and $T = 25.0$ °C.

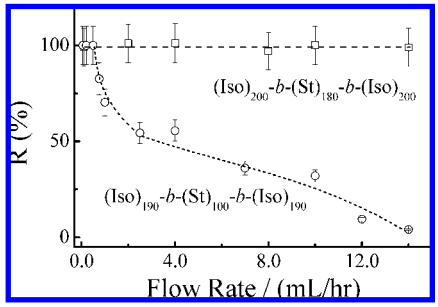

Figure 8. Macroscopic flow-rate dependence of retention ratio of polymeric core−shell micelles made of $(Iso)_{190}$-*b*-$(St)_{100}$-*b*-$(Iso)_{190}$ and $(Iso)_{200}$-*b*-$(St)_{180}$-*b*-$(Iso)_{200}$ in *n*-hexane at 25.0 °C.

Each B block can undergo the intrachain contraction before it associates and interacts with other collapsed B blocks or entangles with other B blocks before it collapses. We found that polymeric micelles made of $(Iso)_{200}$-*b*-$(St)_{180}$-*b*-$(Iso)_{200}$ are completely retained by the filter even under the fastest flow rate available in our current setup. Therefore, we have to shorten the PS block length to reduce the interaction and entanglements inside the core.

Figure 7 shows the flow-rate dependence of hydrodynamic radius distributions of $(Iso)_{190}$- *b*-$(St)_{100}$-*b*-$(Iso)_{190}$ in *n*-hexane after the ultrafiltration. When the flow rate is lower than 0.50 mL/h, there is only one peak in $f(R_h)$, attributed to small $(Iso)_{190}$-*b*-$(St)_{100}$-*b*- $(Iso)_{190}$ unimers because polymeric micelles are retained by the filter. As the flow rate increases, the peak attributed to polymeric micelles appears, indicating that some polymeric micelles are broken and re-formed after individual copolymer chains are pulled out of polymeric micelles and through small pores. The area ratio of these two peaks (A_{mic}/A_{uni}) increases with the flow rate. As stated before, A_{mic}/A_{uni} is directly related to the retention ratio ($R(\%)$).

Figure 8 shows that polymeric micelles are retained when the flow rate is lower than 0.50 mL/h because of a weak hydrodynamic force. In this situation, only unimers free in the solution can pass through small pores, namely, small unimers are separated from large polymeric micelles as long as the exchange time between unimers free in the solution and the copolymer chains bound inside polymeric micelles is longer than our experimental time. By measuring the unimer concentration after the ultrafiltration, we are able to directly estimate the CMC. Our results showed that such an estimated CMC (3.7×10^{-4} g/mL) under a low flow rate (0.1 mL/h) for $(Iso)_{190}$-*b*-$(St)_{100}$-*b*-$(Iso)_{190}$ triblock copolymer in *n*-hexane is fairly close to 2.0×10^{-4} g/mL determined by a traditional LLS method. Note that, when using conventional methods, such as light scattering, surface tension, and fluorescence/dye solubilization, to determine a CMC for a given block copolymer solution, one has to prepare

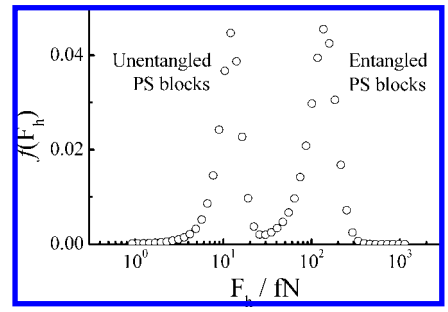

Figure 9. Distribution of hydrodynamic force ($f(F_h)$) required to rupture polymeric micelles made of $(Iso)_{190}$-*b*-$(St)_{100}$-*b*-$(Iso)_{190}$ in *n*-hexane at 25.0 °C.

a series of polymer solutions with different concentrations and measure the concentration dependence of some physical properties.[1,44−48] The extrapolation of measured physical properties to mark its sudden change as CMC is a tricky business, often involving large uncertainties. Using the ultrafiltration, we only need one solution and no extrapolation.

Figure 8 also shows that the retention starts to decrease as the flow rate further increases, indicating that the hydrodynamic force applied to each arm is sufficiently strong to overcome the interaction of the insoluble PS blocks in the core so that individual triblock copolymer chains are pulled out of each polymeric micelle. The continuous decrease of the retention ratio also reflects that the interaction strength of the insoluble PS blocks in the core has a broad distribution. Again, we can take a differentiation of Figure 8 and convert $R(\%)$ to $f(F_h)$.

Figure 9 shows such a distribution of the hydrodynamic force required to rupture polymeric micelles made of $(Iso)_{190}$-*b*-$(St)_{100}$-*b*-$(Iso)_{190}$ in *n*-hexane at 25.0 °C. Surprisingly, $f(F_h)$ has a bimode distribution with two peaks located at ∼10 and ∼100 fN. A possible explanation is as follows. For a PI-*b*-PS-*b*-PI triblock copolymer with an insoluble PS block, the insoluble PS blocks have two different possible kinds of chain packing in the core. Namely, if each PS block collapses before they interact with one another, there is no entanglement among different PS blocks, just like in the case of PS-*b*-PI diblock chains. On the other hand, if different PS blocks are entangled during the collapsing process, it must be more difficult to pull those interwinding chains out of each micelle. Therefore, we can attribute the peak located at ∼10 fN to those interacted chains without any entanglement, and the peak located at ∼100 fN to those chains with their PS blocks entangled with one another. From the area ratio of these two peaks, we can evaluate that ∼50% insoluble PS blocks are entangled with one another inside the core. In comparison with $(Iso)_{190}$-*b*-$(St)_{100}$-*b*-$(Iso)_{190}$, we realize that most of the insoluble PS blocks of $(Iso)_{200}$-*b*-$(St)_{180}$-*b*-$(Iso)_{200}$ must entangle with one another inside the core. This explains why we were not able to pull individual copolymer chains out even under the maximum available flow rate.

Conclusions

After studying the flow-rate-dependent retention of polymeric core−shell micelles made of block copolymers in a selective solvent through small pores (20 nm) in an ultrafiltration experiment, we are able, for the first time, to estimate the distribution of hydrodynamic force [$f(F_h)$] required to pull individual copolymer chains out and rupture each micelle. Such a force distribution in the range $1-10^3$ fN directly reflects the distribution of the interaction strength among the insoluble blocks in the core. Our results show that both the lengths of the soluble and insoluble blocks strongly affect $f(F_h)$. If the insoluble PS block is too long or the soluble PI block is too short, polymeric micelles cannot be disintegrated even under

the fastest flow (100 mL/h) available in our current ultrafiltration setup. For PS-*b*-PI diblock copolymers with a longer soluble PI block in *n*-hexane, $f(F_h)$ has only one peak in the range 1−200 fN. For $(Iso)_{190}$-*b*-$(St)_{100}$-*b*-$(Iso)_{190}$ in *n*-hexane, there exist two peaks in $f(F_h)$ located at ∼10 and ∼100 fN, attributed to the van der Waals interaction among unentangled and entangled insoluble PS blocks in the core. Our results also reveal that, in this case, ∼50% of insoluble PS blocks are entangled with each other in the core.

Acknowledgment. The financial support of the Hong Kong Special Administration Region (HKSAR) Earmarked Project (CU-HK4037/07P, 2160331 and 2060339) and the National Natural Scientific Foundation of China (NNSFC) Project (20574065) are gratefully acknowledged.

References and Notes

(1) Riess, G. *Prog. Polym. Sci.* **2003**, *28*, 1107.
(2) Hadjichristidis, N.; Pispas, S.; Floudas, G. A. *Block Copolymers: Synthetic Strategies, Physical Properties, and Applications*; Wiley & Sons: Hoboken, NJ, 2003.
(3) Hamley, I. W. *The Physics of Block Copolymers*; Oxford University Press: New York, 1998.
(4) Nie, T.; Zhao, Y.; Xie, Z. W.; Wu, C. *Macromolecules* **2003**, *36*, 8825.
(5) Spacek, P.; Kubin, M. *J. Appl. Polym. Sci.* **1985**, *30*, 143.
(6) Booth, C.; Naylor, T. D.; Price, C.; Rajab, N. S.; Stubbersfield, R. B. *J. Chem. Soc., Faraday Trans. 1* **1978**, *74*, 2352.
(7) Price, C.; Hudd, A. L.; Booth, C.; Wright, B. *Polymer* **1982**, *23*, 650.
(8) Benner, R.; Pakulski, J. D.; McCarthy, M.; Hedges, J. I.; Hatcher, P. G. *Science* **1992**, *255*, 1561.
(9) Milligan, K. L. D.; Cosper, E. M. *Science* **1994**, *266*, 805.
(10) Cole-Hamilton, D. J. *Science* **2003**, *299*, 1702.
(11) Jonsson, A. S.; Tragardh, G. *Desalination* **1990**, *77*, 135.
(12) van Reis, R.; Zydney, A. *Curr. Opin. Biotechnol.* **2001**, *12*, 208.
(13) Ferry, G. D. *Chem. Rev.* **1936**, *18*, 373.
(14) Nakao, S. *J. Membr. Sci.* **1994**, *96*, 131.
(15) Zhang, W. M.; Gao, J.; Wu, C. *Macromolecules* **1997**, *30*, 6388.
(16) Siu, M.; Zhang, G. Z.; Wu, C. *Macromolecules* **2002**, *35*, 2723.
(17) Jin, F.; Wu, C. *Phys. Rev. Lett.* **2006**, *96*, 237801.
(18) Nguyen, Q. T.; Neel, J. *J. Membr. Sci.* **1983**, *14*, 111.
(19) Halperin, A.; Tirrell, M.; Lodge, T. P. *Adv. Polym. Sci.* **1992**, *100*, 31.
(20) Birshtein, T. M.; Zhulina, E. B. *Polymer* **1989**, *30*, 170.
(21) Cogan, K. A.; Gast, A. P.; Capel, M. *Macromolecules* **1991**, *24*, 6512.
(22) Zhulina, E. B.; Adam, M.; LaRue, I.; Sheiko, S. S.; Rubinstein, M. *Macromolecules* **2005**, *38*, 5330.
(23) Gast, A. P. *Langmuir* **1996**, *12*, 4060.
(24) Hadjichristidis, N.; Iatrou, H.; Pispas, S.; Pitsikalis, M. *J. Polym. Sci., Part A: Polym. Chem.* **2000**, *38*, 3211.
(25) Uhrig, D.; Mays, J. W. *J. Polym. Sci., Part A: Polym. Chem.* **2005**, *43*, 6179.
(26) Hong, L. Z.; Zhu, F. M.; Li, J. F.; Ngai, T.; Xie, Z. W.; Wu, C. *Macromolecules* **2008**, *41*, 2219.
(27) Ndoni, S.; Papadakis, C. M.; Bates, F. S.; Almdal, K. *Rev. Sci. Instrum.* **1995**, *66*, 1090.
(28) Ren, Y.; Lodge, T. P.; Hillmyer, M. A. *Macromolecules* **2000**, *33*, 866.
(29) Jin, F.; Wu, C. *Acta Polym. Sin.* **2005**, 486.
(30) Chu, B. *Laser Light Scattering: Basic Principles and Practice*; Academic Press: Boston, 1991.
(31) Berne, B. J.; Pecora, R. *Dynamic Light Scattering: With Applications to Chemistry, Biology, and Physics*; Dover Publications: New York, 2000.
(32) Wu, C.; Gao, J. *Macromolecules* **2000**, *33*, 645.
(33) Prochazka, K.; Kiserow, D.; Ramireddy, C.; Tuzar, Z.; Munk, P.; Webber, S. E. *Macromolecules* **1992**, *25*, 454.
(34) Schillen, K.; Yekta, A.; Ni, S.; Winnik, M. A. *Macromolecules* **1998**, *31*, 210.
(35) Rager, T.; Meyer, W. H.; Wegner, G. *Macromol. Chem. Phys.* **1999**, *200*, 1672.
(36) Spevacek, J. *Makromol. Chem. Rapid Commun.* **1982**, *3*, 697.
(37) Kriz, J.; Brus, J.; Plestil, J.; Kurkova, D.; Masar, B.; Dybal, J.; Zune, C.; Jerome, R. *Macromolecules* **2000**, *33*, 4108.
(38) Zhang, L.; Eisenberg, A. *Science* **1995**, *268*, 1728.
(39) Won, Y.; Davis, H. T.; Bates, F. S. *Macromolecules* **2003**, *36*, 953.
(40) Wu, C.; Zhou, S. Q. *Macromolecules* **1995**, *28*, 8381.
(41) Antonietti, M.; Heinz, S.; Schmidt, M.; Rosenauer, C. *Macromolecules* **1994**, *27*, 3276.
(42) Jones, J. L.; Marques, C. M.; Joanny, J. F. *Macromolecules* **1995**, *28*, 136.
(43) Cai, P.; Wang, C. Q.; Ye, J.; Xie, Z. W.; Wu, C. *Macromolecules* **2004**, *37*, 3438.
(44) Gohy, J. F. *Adv. Polym. Sci.* **2005**, *190*, 65.
(45) Khougaz, K.; Gao, Z. S.; Eisenberg, A. *Macromolecules* **1994**, *27*, 6341.
(46) Alexandridis, P.; Holzwarth, J. F.; Hatton, T. A. *Macromolecules* **1994**, *27*, 2414.
(47) Wilhelm, M.; Zhao, C. L.; Wang, Y. C.; Xu, R. L.; Winnik, M. A.; Mura, J. L.; Riess, G.; Croucher, M. D. *Macromolecules* **1991**, *24*, 1033.
(48) Li, M.; Jiang, M.; Wu, C. *J. Polym. Sci., Part B: Polym. Phys.* **1997**, *35*, 1593.

MA801702T